RESEARCH ARTICLE

WILEY

Frequency scan analysis supported by a possibility theory-based approach

Andrés Arturo Romero Quete [ID] | Joaquín Eduardo Caicedo Navarro [ID] |
Humberto Cassiano Zini | Giuseppe Rattá [ID]

Instituto de Energía Eléctrica, Facultad de ingeniería, Universidad Nacional de San Juan—CONICET, San Juan, República Argentina

Correspondence
Joaquín Eduardo Caicedo Navarro, Instituto de Energía Eléctrica, Facultad de ingeniería, Universidad Nacional de San Juan—CONICET, Av. Libertador General San Martín Oeste 1109, J5400ARL, San Juan, República Argentina.
Email: jcaicedo@iee.unsj.edu.ar

Summary

This paper describes a procedure used to identify the states of a power system that lead to harmonic resonance. The proposed methodology results from an application of the possibility theory which aims to extend the capabilities of the classic frequency scan concept. With the proposed approach, the frequency scan provides more useful information on the harmonic behavior of a power system in contexts where load characteristics are known with uncertainty. To exemplify the potential of this proposal, a case study based on a 14-bus standard test system for harmonic analysis is presented. The states of the power system that lead to harmonic resonance are assessed within the possibility theory framework. Additionally, this paper introduces a risk measure of harmonic resonance based on possibility and necessity fuzzy measures.

KEYWORDS

frequency scan, harmonic distortion, possibility theory, power quality, resonance

1 | INTRODUCTION

Harmonic resonance is a major concern for utilities and power engineers. It is caused by the energy exchange between capacitive and inductive elements in the electric power system,[1] leading to low impedance (series resonance) or high impedance (parallel resonance) to the flow of harmonic currents.[2] Consequently, harmonic distortion levels are amplified. The magnified harmonics have severe negative impacts on the power system, eg, maloperation of protective devices, derating of equipment, and damage of shunt capacitors.[3] Therefore, the analysis of harmonic resonance is of paramount importance for planning power networks and implementing mitigation measures.

Few approaches are available to perform harmonic resonance analysis, namely: mode analysis[1] and frequency scan.[4,5] The latter is the most widely used because of its simplicity and minimum input data requirement.[4] This frequency scan analysis is used to characterize the frequency response of an electrical network, ie, to determine how the network impedance, seen from a specific node, varies as a function of frequency. To that end, repeated solutions of a linear system of equations, which relates injected currents to the nodal admittance matrix and voltages, are computed for each frequency of interest. In particular, it is a useful tool for examining the system response to harmonic currents injected by nonlinear loads.[4] Some applications of the frequency scan include the analysis of resonance in unbalanced distribution networks,[6] wind parks,[7,8] AC traction systems,[9] passive filters,[10] and photovoltaic inverters.[11]

LIST OF SYMBOLS: x, real scalar; $\mathbf{U}$, real vector or matrix; X, classic set; $\widehat{X}$, fuzzy set or fuzzy number; $\mu_{\widehat{X}}$, membership function of the fuzzy set $\widehat{X}$; α, α-value of a fuzzy set, membership degree; $X^{(\alpha)}$, α-cut set of the fuzzy set $\widehat{X}$; $\underline{x}^{(\alpha)}$, lower boundary of an α-cut set; $\overline{x}^{(\alpha)}$, upper boundary of an α-cut set

Moreover, commercially available and open simulation tools for harmonic analysis usually include frequency scan capabilities.[12-14]

Despite its simple application and widespread use, frequency scan analyses usually lack considerations of uncertainties related to the frequency response of the power system. Although the electrical grid configuration to be analyzed can often be assumed to be invariant within the scope of a specific study during a defined period of time, loads supplied by the grid continuously vary in somewhat unpredictable ways. Likewise, the composition of loads (percentage of rotating and static, linear and nonlinear) is known with uncertainty related to lack of knowledge and imprecision. Both features, load magnitude and composition, affect the frequency response. To deal with the aforementioned uncertainty, frequency scans are usually performed for those load conditions regarded as the most probable or critical, based on engineering judgment.[15,16] However, at present, there are no systematic methods for predicting harmonic resonance in large power grids.[17] In this context, if one is seeking more reliable results, uncertainty should be suitably modeled by using methods of probability theory[8,10,15,16,18-20] or as is proposed in this paper, by resorting to the possibility theory.[21-23]

Considering uncertainties in the frequency response is essential for making a decision to implement a mitigation measure for harmonic resonance in a power network.[15] For instance, in the design of passive harmonic filters, or in shunt capacitors sizing, for power factor correction, the risk of resonance should be quantified. As regards this issue, it is worth noting that ISO 31000:2009[24] indicates that risk can be expressed in terms of a combination of the consequences of an event (severity) and the associated likelihood of occurrence.

In this paper, it will be shown that possibility theory offers an adequate framework to deal with incomplete knowledge in loads that affect the harmonic performance of an electrical network. In particular, it will be shown that possibility and necessity measures, instead of probabilistic measures, allow for a more realistic valuation of uncertainty related to the harmonic resonance phenomenon. The key idea of the proposed methodology is to adapt the conventional frequency scan to a possibility-based approach. With the outlined methodology, a set of meaningful frequency response curves are obtained, improving the reliability of the harmonic studies. In fact, the proposed approach yields the minimum and maximum driving point impedance, as the system loads change. Thus, the range of all possible resonant points is estimated for a given period of study.

Moreover, a risk of resonance index is proposed in this paper based on the possibility measures of parallel resonance and the severity of the event. This index would be useful for decision-making on harmonic resonance mitigation measures.

In synthesis, the contributions of this paper are the following:

1. A novel approach for analyzing the harmonic resonance phenomenon, based on possibility theory to deal with uncertainties associated with variation and composition of loads. The approach yields useful frequency response curves used to identify the possibility of resonance and its severity. Unlike current approaches for harmonic resonance analysis, this methodology allows for calculating the range in magnitude of all possible driving point impedances.
2. A risk of resonance index for decision-making, based on possibility and necessity fuzzy measures.

This paper is organized as follows. In Section 2, the theoretical frameworks regarding frequency scan analysis and possibility theory are presented. Section 3 introduces the methodology for the possibilistic calculation of the driving point and transfer impedances. In Section 4, the models implemented for characterizing the uncertainties of load impedances are detailed. The proposed methodology is outlined in Section 5, and its capability is demonstrated in Section 6 through a case study developed in a 14-bus standard test system for harmonic analysis. Finally, results are discussed, and conclusions are drawn.

2 | THEORETICAL FRAMEWORK

2.1 | Frequency scan analysis

Frequency scan analysis is used to characterize the response of a power system as a function of frequency. It is conducted through repeated solutions of the linear system of equations expressed in Equation 1, for a set of frequencies, in an interval of interest.

$$\mathbf{I} = \mathbf{Y}_{bus}(f)\mathbf{U} \tag{1}$$

In Equation 1, $\mathbf{U}$ and $\mathbf{I}$ are vectors of node voltages and injected currents at frequency f, which are related through the nodal admittance matrix, $\mathbf{Y}_{bus}$ (f), calculated at the corresponding frequency. Frequency scan is usually based on a single current injection into the power system. For $I_i = 1\llcorner 0°$ A, and $I_k = 0$ for $k \neq i$, the solution to Equation 1 determines the voltages per unit current at every bus of the network, due to the current injected at bus i. The calculated voltages also represent the driving point and transfer impedances as seen at node i, because of the unitary value of I_i. The model only contains linear elements; therefore, linearity can be applied to scale the results obtained for $1\llcorner 0°$ A, to any desired value. This scalability can be applied in order to estimate the harmonic voltages that will be produced at any bus of the network when a nonlinear load is connected at the injection node i.[5]

2.2 | Fuzzy sets and the alpha cut concept

In fuzzy set theory, the membership function $\mu_{\widehat{A}}$ of the fuzzy set $\widehat{A}$ maps elements x of a given universal set X into the real interval [0, 1].

$$\mu_{\widehat{A}}: X \rightarrow [0, 1] \tag{2}$$

Fuzzy sets where elements of X are real numbers are known as fuzzy numbers.[25] Figure 1 shows a generic fuzzy number that can also be seen as a sequence of nested confidence intervals called α-cuts, ie, $A^{(\alpha)} = \left[\underline{x}^{(\alpha)}, \overline{x}^{(\alpha)}\right]$.

2.3 | Possibility theory

In the most common applications currently, the membership function of a fuzzy set indicates the degree to which an element of the universal set belongs to a subset with non-well-defined limits. In this paper, however, fuzzy sets, and more specifically fuzzy numbers, are used as fuzzy measures in the context of possibility theory. In this context, a fuzzy variable with its membership function is related to a possibility distribution.[21-23]

Possibility theory is based on 2 dual non-additive measures called necessity (*nec*) and possibility (*pos*).[25] For finite universal sets, the possibility measure is formally expressed as

$$pos(S) = \max_{x \in S} \left(\mu_{\widehat{A}}(x)\right) \tag{3}$$

and the necessity measure as

$$nec(S) = 1 - \max_{x \notin S} \left(\mu_{\widehat{A}}(x)\right) \tag{4}$$

for each $S \in P(X)$. $P(X)$ is defined as the power set of all classic subsets on the universe X.
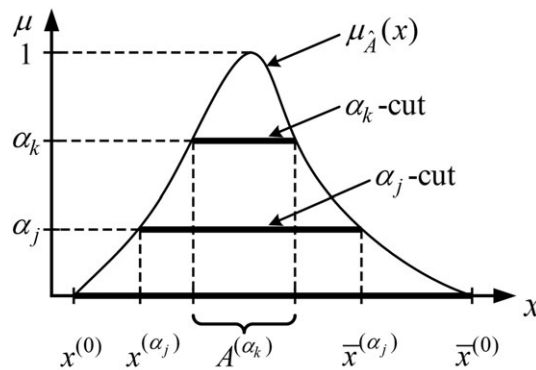

FIGURE 1 Representation of the membership function of a fuzzy number $\widehat{A}$

As can be seen in Figure 1, *nec* is maximum for $A^{(0)}$ (ie, $nec(A^{(0)}) = 1$) because it is completely certain that the value of the magnitude is within the 0-cut and decreases as α increases (shorter α-cuts). The membership function $\mu_{\widehat{A}}$, used to quantify the uncertainty in a parameter A in possibility theory, is called the possibility distribution of A.

Another issue in possibility theory is possibilistic interaction. To some extent, this concept is analogous to conditional probability. It arises when 2 or more uncertain parameters, whose possibilities are estimated somewhat independently, are linked through a well-defined physical relationship. As an example, consider that the linear (P_l), nonlinear (P_{nl}), and total load (P_t) could be independently estimated as 0.5 MW $< P_l <$ 0.8 MW, 0.2 MW $< P_{nl} <$ 0.4 MW and 0.8 MW $< P_t <$ 1.1 MW, but the constraint $P_t = P_l + P_{nl}$ defines a possibilistic interaction among them. A more detailed analysis of possibilistic interaction in the context of harmonic analysis can be found in a previous study.[26]

3 | POSSIBILISTIC EVALUATION OF THE DRIVING POINT AND TRANSFER IMPEDANCES

In the developed model, most loads are known with uncertainty. Clearly, such uncertainty propagates to the driving point and transfer impedances. The methodology described in this section allows for quantifying the uncertainties in the impedances when the possibility distribution functions of the uncertain parameters are given.

For this purpose, let $\mathbf{P} = [p_1, p_2,...,p_{np}]$ be a vector of n_p real parameters that completely define the uncertain bus loads. At a specific frequency or harmonic order, the bus admittance matrix can be expressed as a function of these parameters, ie,

$$\mathbf{Y}_{bus} = \mathbf{Y}(f, \mathbf{P}) \tag{5}$$

More specifically, because loads are modeled as branches connected to ground, only the diagonal elements of $\mathbf{Y}_{bus}$ corresponding to busses with uncertain loads will depend on some or all p_k, $k = 1...n_p$. Conversely, in general, each parameter influences all driving point and transfer impedances, making the voltage magnitude at any bus j per unit current injected at a bus k, a function of all of them:

$$v_{j,k} = \left| \mathbf{z}_{j,k}(f, \mathbf{P}) \right| \tag{6}$$

where, $\mathbf{z}_{j,k}$ are the elements of $\mathbf{Z}_{bus} = \mathbf{Y}_{bus}^{-1}$.

Parameters p_k are known with uncertainties quantified by possibility distribution functions $\mu_{\widehat{P_k}}(p_k)$, $k = 1...n_p$.

In addition, possibilistic interaction could exist among them (eg, active load due to linear and nonlinear devices must add up to the total active load), a situation generally described through a system of $n_d < n_p$ equations in terms of $n_i = n_p - n_d$ independent parameters, ie,

$$\begin{aligned} p_{n_i+1} &= g_1\left(p_1, p_2, ..., p_{n_i}\right) \\ &\vdots \\ p_{n_i+n_d} &= g_{n_d}\left(p_1, p_2, ..., p_{n_i}\right) \end{aligned} \tag{7}$$

The relationship between the possibility distribution functions of the voltages per unit currents, $\mu_{\widehat{V_{j,k}}}(v_{j,k})$, and those of the uncertain load parameters $\mu_{\widehat{P_k}}(p_k)$, $k = 1...n_p$, can be easily stated in terms of their corresponding α-cuts. Specifically, as shown in Equations 8 to 10, the α-cut of a voltage per unit current is the interval spanned by the magnitude of the corresponding impedance when the loads vary within the limits allowed by the corresponding α-cuts of their uncertain parameters.

$$u_{j,k}^{(\alpha)}(f) = \left[\underline{u}_{j,k}^{(\alpha)}(f), \overline{u}_{j,k}^{(\alpha)}(f) \right] \tag{8}$$

With:

$$
\begin{aligned}
\underline{u}_{j,k}^{(\alpha)}(f) &= \min \left| \mathbf{z}_{j,k}\left(f, p_1, .., p_{n_p}\right) \right| \\
\overline{u}_{j,k}^{(\alpha)}(f) &= \max \left| \mathbf{z}_{j,k}\left(f, p_1, .., p_{n_p}\right) \right|
\end{aligned}
\tag{9}
$$

Both subject to:

$$
\begin{cases}
\underline{p}_1^{(\alpha)} \leq p_1 \leq \overline{p}_1^{(\alpha)} \\
\quad\vdots \\
\underline{p}_{n_{p}^{(\alpha)}} \leq p_{n_p} \leq \overline{p}_{n_{p}^{(\alpha)}} \\
p_{n_i+1} = g_1\left(p_{n_1}..p_{n_i}\right) \\
\quad\vdots \\
p_{n_i+n_d} = g_{n_d}\left(p_{n_1}..p_{n_i}\right)
\end{cases}
\tag{10}
$$

Hence, to determine each α-cut of $u_{j,k}$, 2 optimization problems are solved; a nonlinear programming routine based on a generalized reduced gradient algorithm was used to solve the constrained maximization and minimization of $\left| \mathbf{z}_{j,k}\left(f, p_1, \cdots, p_{n_p}\right) \right|$.

The efficiency of the optimization procedure is greatly increased by providing the partial derivatives of the objective function $|\mathbf{z}_{j,k}|$, which are evaluated with low computational effort through the following expression:

$$
\frac{\partial |\mathbf{z}_{j,k}|}{\partial p_i} = \operatorname{Re}\left(-\frac{|\mathbf{z}_{j,k}|}{\mathbf{z}_{j,k}} \left[\mathbf{z}_{j,1} \cdots \mathbf{z}_{j,n} \right] \begin{bmatrix} \partial \mathbf{y}_{1,0}/\partial p_i & 0 & 0 \\ 0 & \ddots & 0 \\ 0 & 0 & \partial \mathbf{y}_{n,0}/\partial p_i \end{bmatrix} \begin{bmatrix} \mathbf{z}_{1,k} \\ \vdots \\ \mathbf{z}_{n,k} \end{bmatrix} \right)
\tag{11}
$$

where $\mathbf{y}_{1,0} \dots \mathbf{y}_{n,0}$ are the total admittances to ground of the branches that model the load connected at the n busses of the power system.

4 | LOAD MODELING

A key aspect in developing a possibilistic model for harmonic analysis is to define a suitable set of parameters p_k, $k = 1...$ n_p, to describe the available uncertain information regarding the load characteristics. In addition, those parameters must completely define the admittance to ground that models the load. Therefore, the main steps for developing the load model are as follows:

1. Define the harmonic load model, ie, a proper RLC circuit to model the harmonic behavior of the loads (in a deterministic sense).
2. Select a set of fuzzy parameters to describe the available information regarding the magnitude and composition of load. This will be referred to as the set of *model parameters*, as opposed to the *circuit parameters* (RLC components of the circuit defined in 1).
3. Establish the relationship between *model parameters* and *circuit parameters*.

In this section, the characteristics of the circuit adopted to model the load will be described.

4.1 | Harmonic load model (circuit parameters)

Standard load models for harmonic load-flow calculation are parallel connections of impedances, representing the linear loads, shunt compensation, and passive filters. Different studies and measurement campaigns suggest the deterministic load model shown in Figure 2,[27] where each branch represents an aggregate of homogeneous loads and the superscript (h) denotes the harmonic order. A brief explanation of the different loads each branch models will now be presented.
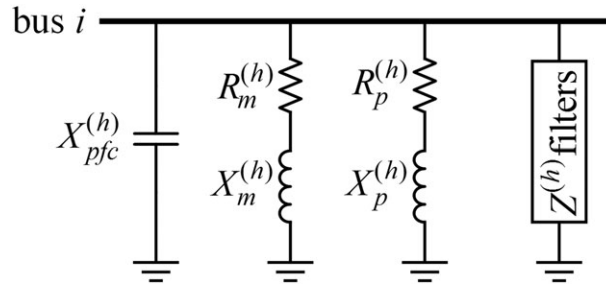
FIGURE 2   Electrical model of loads for harmonic analysis

4.1.1 | Passive (non-rotating) linear loads

Series resistance $R_p^{(h)}$ and inductance $X_p^{(h)}$ model passive (non-rotating) linear loads and small motors (appliances). For loads at a lower voltage level, the main component of inductance $X_p^{(h)}$ is the short circuit inductance of the distribution transformer. Skin and proximity effects are taken into account through a factor $\sqrt{h}$ (ie, $R_p^{(h)} = \sqrt{h}R_p^{(1)}$).

4.1.2 | Motive loads

Circuit parameters $R_m^{(h)}$ and $X_m^{(h)}$ model large motors used in industrial applications. $X_m^{(h)} = hX_{LR}$, where X_{LR} is the locked rotor reactance and R_m is regarded for the harmonic attenuation which depends mainly on the quality factor of the rotor circuit. Slightly more sophisticated models (with higher accuracy mainly at harmonic orders below the fifth) could also be implemented.[5]

4.1.3 | Capacitive loads

Capacitive reactance $X_{pfc}^{(h)} = X_{pfc}^{(1)}/h$ models the capacitors for power factor correction and cable capacitance when relevant.

4.1.4 | Harmonic filters

Harmonic filters are usually associated with large nonlinear loads, and their parameters are usually well known (non-fuzzy). Consequently, the branches modeling them in Figure 2 are included among the network parameters, such as line and transformer impedances or capacitive compensation installed by the utility, which are certain.

4.2 | Model parameters to be described by possibility distributions

Some electrical parameters of the load model in Figure 2 are uncertain, and, in principle, might be described through their possibility distribution functions. However, in practice, the available information usually refers to other load features, such as its total active and reactive power, its percentage due to linear and nonlinear devices, etc. Different sets of model parameters could be selected. Table 1 summarizes the authors' choice. The relationships between model parameters in Table 1 and circuit parameters in Figure 2 are presented in the appendix of a previous work.[28]

  The possibility distribution functions of the load model parameters are usually defined by taking into account the expected value of the active and reactive loads, estimations of their maximum deviations, and some expert judgment regarding their composition.

  In the case study in Section 6, triangular distributions have been assumed with the maximum at the expected value and the limits of the 0-cut defined by the maximum estimated deviation. The reason for selecting triangular distributions (in a possibility theory-based approach) is founded on the fact that these are genuine counterparts of normal probability densities (in a probability theory-based approach).[29] This finding makes this type of distribution useful for most practical applications. However, it is worth noting that the proposed approach allows for the use of possibility distributions with other shapes (eg, gaussian, trapezoidal, etc.), if required, because the method relies on the α-cut concept.

TABLE 1 Uncertain load parameters for the harmonic analysis

Model Parameter	Description
$P_{t,i}$	Total active power at fundamental frequency at node i
$Q_{t,i}$	Total reactive power at fundamental frequency at node i
$K_{p,i}$	Composition factor of passive loads (fraction of the passive load in the total active bus load) at node i
$pf_{p,i}$	Power factor of passive loads at node i
$K_{m,i}$	Composition factor of motive loads (fraction of the motive load in the total active bus load) at node i
$pf_{m,i}$	Power factor of motive loads at node i
$K_{nl,i}$	Composition factor of nonlinear load(s) (fraction of the nonlinear load in the total active bus load) at node i
$pf_{nl,i}$	Power factor of nonlinear load(s) at node i
x_{LR}	Locked rotor reactance in pu (x_{LR} typically ranges from 0.15 to 0.25 pu)
$Q_{pfc,i}$	Reactive power due to the capacitors for power factor correction, at fundamental frequency, at node i

# 5 | PROCEDURE FOR FREQUENCY SCAN ANALYSIS BASED ON THE POSSIBILISTIC APPROACH

The key idea of the proposed methodology is to use results from the possibilistic calculation outlined in Section 3 to select, on a rational basis, specific values of the load parameters to carry out the frequency scan calculations.

The methodology presented in Section 3 allows to obtain possibility distribution functions of the bus voltage per unit current at any frequency. If the method is applied for a large set of frequencies, a full possibilistic frequency scan is obtained. This concept is illustrated in Figure 3, where possibility distributions of a bus voltage per unit current at 6 frequencies (f_1, f_2, f_3, f_4, f_5, and f_6) are shown. The contour lines are the loci of the voltages per unit current with equal possibility at different frequencies.

Although interesting, the full possibilistic frequency scan entails high computational effort and lacks the useful physical meaning of the frequency responses obtained with the classic frequency scan, described in Section 2.1. For instance, as optimizing parameters in Equations 8 to 10 depends on the frequency, the system loads vary along the contour lines (except for $\alpha = 1$), making them different from the classic frequency response curves.

In order to overcome these drawbacks, a slightly different approach is proposed. It arises from the recognition that, usually, the main concern in harmonic studies is the frequency response near some characteristic harmonic orders (eg, the characteristic harmonics of 6 pulse rectifiers). Taking this into account, a 2-step procedure is proposed for each relevant harmonic order.

In the first stage, possibility distribution of the voltage per unit current is computed for the relevant harmonic order. Specifically, a suitable set of α-cuts, including the 0-cut and 1-cut, are calculated. In the optimization process, Equations 8 to 10, both the limits of each α-cut and the corresponding optimizing load parameters are computed and stored.
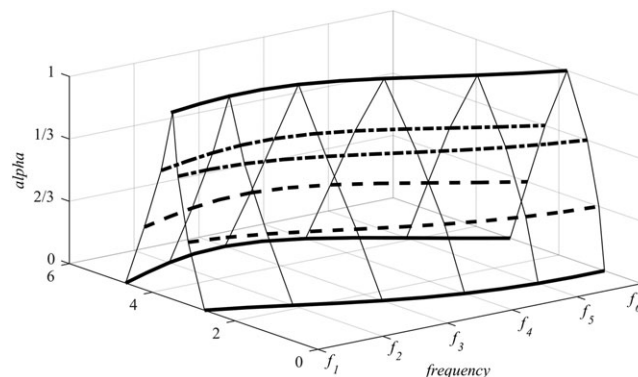
FIGURE 3 Diagram of curves associated with a full possibilistic frequency scan

In the second stage, classic frequency scans are computed with the optimizing load parameters related to each α-cut. The following features should be noted:

1. Unlike the contour lines of the full possibilistic frequency scan, the obtained curves are the frequency responses of the system with specific load parameters. In general, they coincide with the contour lines only at the relevant harmonic frequencies.
2. Curves for the same α-cut but different frequency do not match because in general they are obtained with different load conditions. Clearly, each curve is relevant near the harmonic frequency from which it has been computed.

The proposed methodology is conveniently illustrated through the case study presented in the next section.

It is worth noting that an analogous methodology based on probability theory does not seem to be feasible. In fact, although probability distributions of load parameters, known with uncertainty, can be obtained objectively or subjectively,[15,16] to be used, for example, in Monte Carlo simulations, there would not be a single randomly generated set of load parameters that leads to the case of parallel resonance with the greater amplitude, ie, it is improbable to randomly tune the power system and its loads in such a resonance state. On the other hand, the possibility methodology performs an optimization process aimed at tuning the power system in resonance frequency, if possible for the range of variation of the uncertain parameters. To assess this last consideration, in the case study Monte Carlo simulations were also performed and were compared with results obtained from the possibility theory-based approach.

6 | CASE STUDY

6.1 | Description of the case study

In this section, the proposed methodology is applied to the IEEE 14-bus harmonic test system. The network diagram and main parameters are summarized by Abu-hashim et al[30] and Romero et al.[28] Generators, lines, and transformers have been modeled according to widely used recommendations for harmonic analyses.[4]

Triangular possibility distribution functions are assumed for the load parameters. Active and reactive power of loads, specified in the 14-bus test system,[30] are used as central values (m) or 1-cut of the distributions. Uncertainty is assumed to be $\pm 5\%$ of such central values. Thus, the 0-cuts of the possibility distributions are the intervals [0.95 m, 1.05 m]. The percentage of induction motors and other linear loads have been chosen quite arbitrarily. The possibility distributions of load parameters are reported in Table 2.
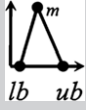
6.2 | Analysis of results

The methodology described in Section 3 was applied to compute the possibility distributions of the voltage per unit current (driving point impedance) at the 14 network busses, for the 5th, 7th, 11th, 13th, 17th, and 19th harmonic orders. Seven α-cuts ($\alpha = k/6$, with $k = 0, 1, ..., 6$) were computed; however, for clarity, only 4 are shown in the figures below. Additional points of the possibility distributions were interpolated when required. Afterwards, the corresponding frequency scans were carried out according to the procedure described in Section 5. The obtained frequency scan curves were then analyzed in order to detect parallel resonance (ie, the voltage per unit current at the local peak) at each studied harmonic order. When a resonance was detected, both possibility and necessity measures were computed by means of Equations 3 and 4. In fact, the possibility measure of a parallel resonance at the harmonic order h, $pos(R_h)$ is equal to the maximum value of α for which the parallel resonance is presented. The necessity measure was calculated similarly.

In Figure 4, possibility distributions obtained for the seventh harmonic voltage per unit current at the 14 busses are reported.

In this case, harmonic resonances were detected. Both possibility and necessity measures, $pos(R_7)$ and $nec(R_7)$, and the maximum magnitude of the resonance, V/A_{max7}, were computed and reported in Table 3.

From Table 3, note that the highest voltage under resonant condition is achieved at bus 14. Another interesting observation for bus 4 reveals that it exhibits the highest necessity measure. This last result means that there is more evidence indicating that the seventh harmonic resonance could occur in this bus, as compared with the rest of the busses. Possible frequency responses for these 2 busses are shown in Figure 5.

TABLE 2 Possibilistic parameter modeling loads connected to the IEEE 14-bus power system

Bus		$P_{t,i}$	$Q_{t,i}$	$K_{p,i}$	$pf_{p,i}$	$K_{m,i}$	$pf_{m,i}$	$K_{nl,i}$	$pf_{nl,i}$	x_{LR}	$Q_{pfc,i}$
3	lb	1.131	0.064	0		0		1	0.8		0.660
	m	1.190	0.067	0		0		1	0.8		0.825
	ub	1.250	0.071	0		0		1	0.8		0.990
4	lb	0.454	-0.037	0.5	0.97	0.2	0.7	0		0.15	0.163
	m	0.478	-0.039	0.7	0.975	0.3	0.8	0		0.2	0.204
	ub	0.502	-0.041	0.9	0.98	0.4	0.9	0		0.25	0.245
5	lb	0.072	0.015	0.55	0.97	0.2	0.8	0		0.15	0.008
	m	0.076	0.016	0.75	0.975	0.25	0.825	0		0.2	0.010
	ub	0.080	0.017	0.95	0.98	0.3	0.85	0		0.25	0.012
8	lb	0.124	0.000	0		0		1	0.8		0.078
	m	0.130	0.000	0		0		1	0.8		0.098
	ub	0.137	0.000	0		0		1	0.8		0.117
9	lb	0.280	0.158	0.5	0.8	0.2	0.7	0		0.15	0.023
	m	0.295	0.166	0.7	0.85	0.3	0.8	0		0.2	0.028
	ub	0.310	0.174	0.9	0.9	0.4	0.9	0		0.25	0.034
10	lb	0.086	0.054	0.5	0.8	0.2	0.8	0		0.15	.00015
	m	0.090	0.057	0.7	0.85	0.3	0.83	0		0.2	.00019
	ub	0.095	0.060	0.9	0.9	0.4	0.86	0		0.25	.00023
11	lb	0.033	0.017	0.5	0.8	0.2	0.8	0		0.15	0.003
	m	0.035	0.018	0.7	0.85	0.3	0.85	0		0.2	0.004
	ub	0.037	0.019	0.9	0.9	0.4	0.9	0		0.25	0.004
12	lb	0.058	0.014	0.5	0.8	0.2	0.7	0		0.15	0.020
	m	0.061	0.015	0.7	0.85	0.3	0.8	0		0.2	0.025
	ub	0.064	0.016	0.9	0.9	0.4	0.9	0		0.25	0.030
13	lb	0.128	0.055	0.5	0.8	0.2	0.8	0		0.15	0.021
	m	0.135	0.058	0.7	0.85	0.3	0.85	0		0.2	0.026
	ub	0.142	0.061	0.9	0.9	0.4	0.9	0		0.25	0.031
14	lb	0.142	0.048	0.3	0.9	0.5	0.8	0		0.15	0.022
	m	0.149	0.050	0.4	0.94	0.6	0.85	0		0.2	0.027
	ub	0.156	0.053	0.5	0.98	0.7	0.9	0		0.25	0.032

The results for the 13th harmonic order are shown in Figure 6. Maximum voltages per unit current, V/A_{max13}, obtained under resonance condition, and both possibility and necessity measures of the occurrence of such resonance are reported in Table 4.

Table 4 reveals that the highest voltage per unit of current under resonance condition is achieved at bus 12. Therefore, the possible frequency response of the network seen from this bus is plotted in Figure 7.

Similarly, possibility distributions of voltage per unit current obtained from the analysis at the 19th harmonic order are shown in Figure 8. Additionally, maximum voltage per unit current achieved under resonance condition and possibility and necessity measures are reported in Table 5. The possible frequency responses for the most critical bus are plotted in Figure 9. Moreover, a comparison with 100 Monte Carlo simulations, randomly generated by using uniform probability distributions with the same boundaries given by the of the 0-cut of the uncertain parameters, ie, [lb, ub] values reported in Table 2, was performed. Results are plotted in Figure 10.

6.3 | Discussion

For the case study, parallel resonance was found impossible to occur at any of the 14 busses for the 5th and 11th harmonic orders. On the contrary, the possibility of parallel resonance was detected for the 7th, 13th, 17th, and 19th harmonic orders, at several busses of the power system.
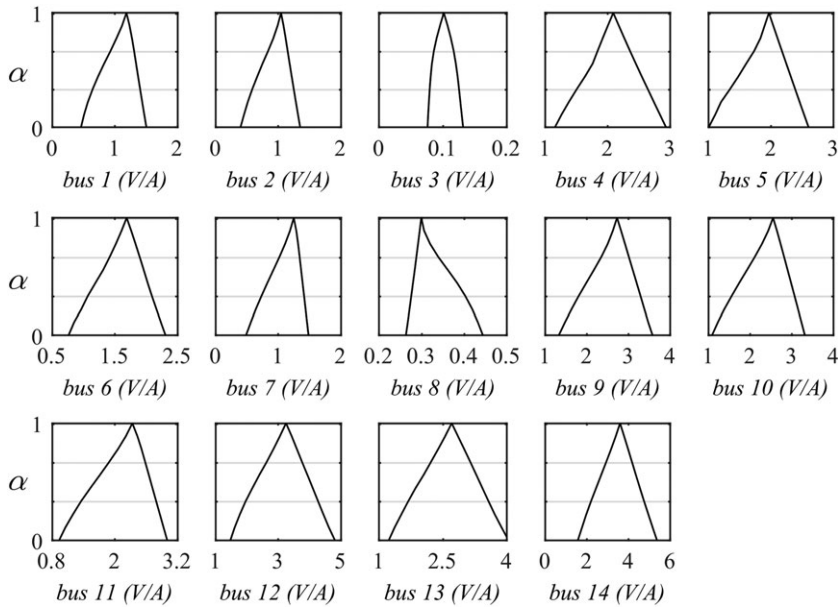
FIGURE 4 Possibility distributions of the seventh harmonic voltage per unit current

TABLE 3 Possibility measures and magnitude of resonances at seventh harmonic order

Bus	1	2	3	4	5	6	7	8	9	10	11	12	13	14
V/A_{max7}	1.50	1.35	0.13	2.93	2.60	2.30	1.48	-	3.57	3.31	3.0	4.8	4.04	**5.37**
$Pos(R_7)$	0.83	1	0.66	1	1	1	1	0	1	1	0.83	0.83	0.83	0.83
$Nec(R_7)$	0	0	0	**0.5**	0.16	0	0.16	0	0.16	0	0	0	0	0

Bold data indicates that bus 4 has the highest value of necessity measure. Bold data indicates that bus 14 has the highest value of driving point impedance.
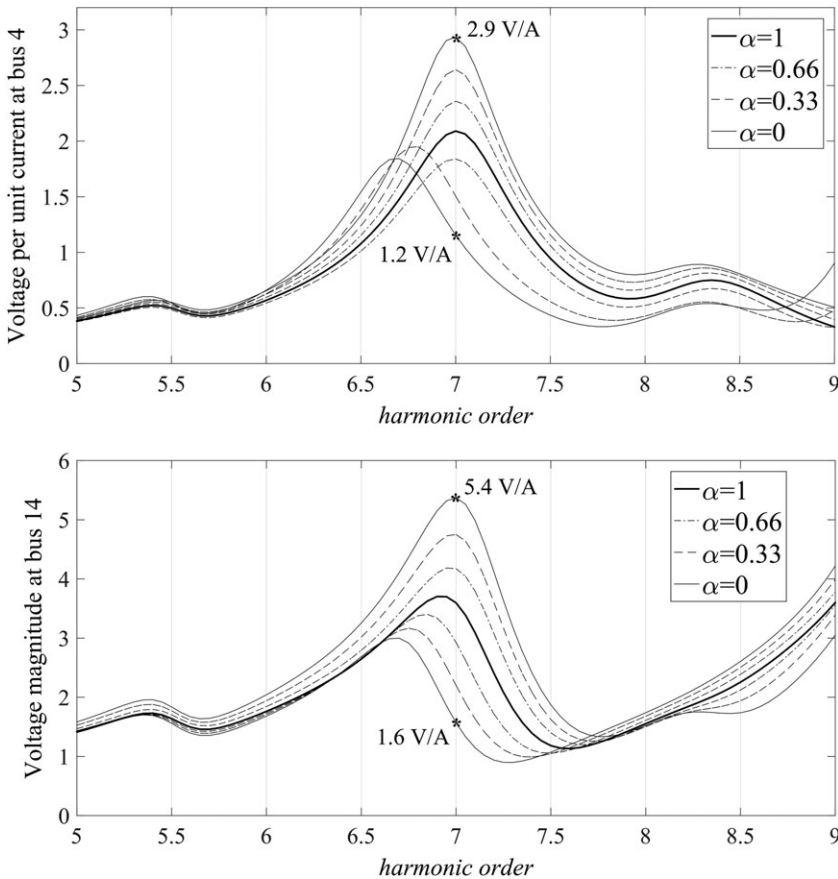

FIGURE 5 Possible frequency response of the network seen from busses 4 and 14
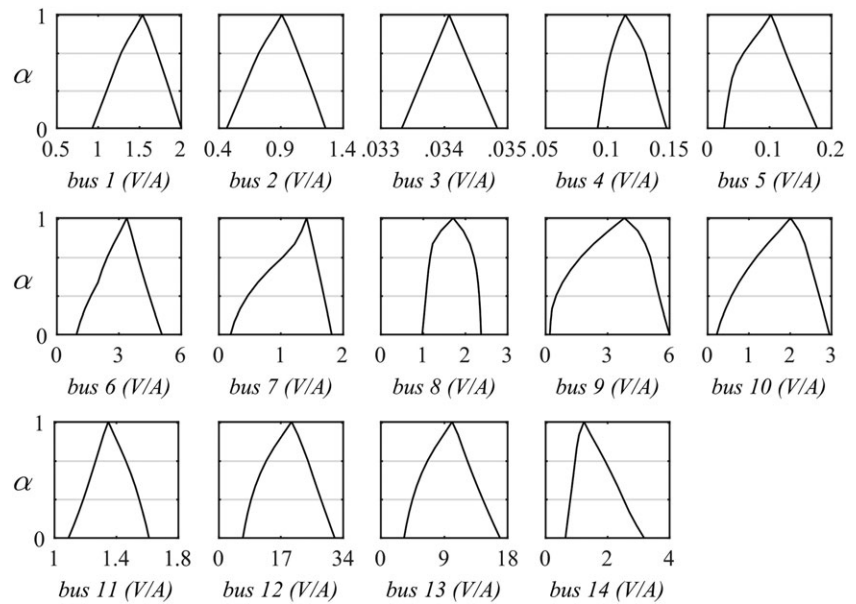
FIGURE 6 Possibility distributions of the 13th-order harmonic voltage per unit current

TABLE 4 Possibility measures and magnitude of resonances at 13th harmonic order

Bus	1	2	3	4	5	6	7	8	9	10	11	12	13	14
V/A_{max13}	-	-	-	-	0.17	5.07	1.81	2.37	5.99	2.95	-	**31.7**	16.9	3.18
$Pos(R_{13})$	0	0	0	0	1	1	1	0.83	0.83	0.83	0	0.83	0.83	0.83
$Nec(R_{13})$	0	0	0	0	0	0	0.16	0	0	0	0	0	0	0

Bold data indicates that bus 12 has the highest value of driving point impedance.

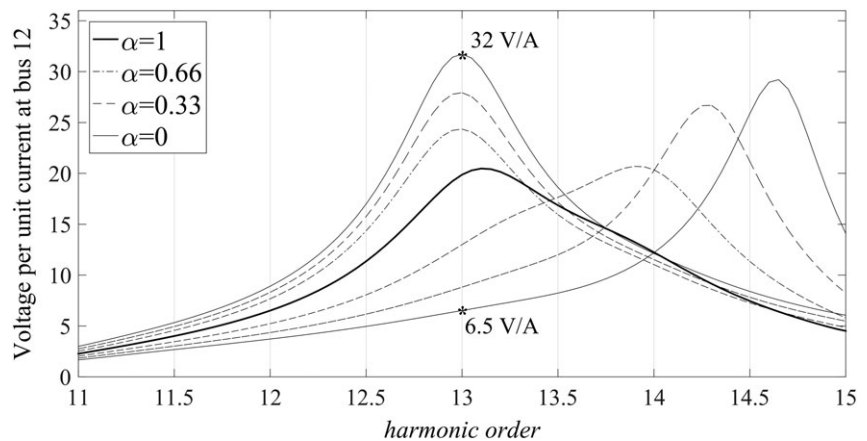**FIGURE 7** Possible frequency response of the network seen from bus 12

As an example, 3 rankings were developed by using results obtained for the 7th and 19th harmonic orders. The first ranking is based on the computed uncertainty measures that indicate the likelihood of resonance occurrence. The second is based on the maximum voltage per unit current reached at resonance. The third ranking is based on a risk index arbitrarily defined in this article as the product of the possibility by the magnitude of the parallel resonance. These 3 rankings are shown in Table 6.

The product of the likelihood of an adverse event by its consequences is a common index in risk assessment (other techniques are, for example, based on the analysis of risk matrices[31]).

Rankings in Table 6 can be useful in decision-making. In particular, such decisions can be founded on specific objectives, eg, to mitigate the risk of resonance or to reduce the maximum possible magnitude of resonance. It is apparent from Table 6 that special care should be taken with busses 12 and 14. Results show that these busses also exhibited high
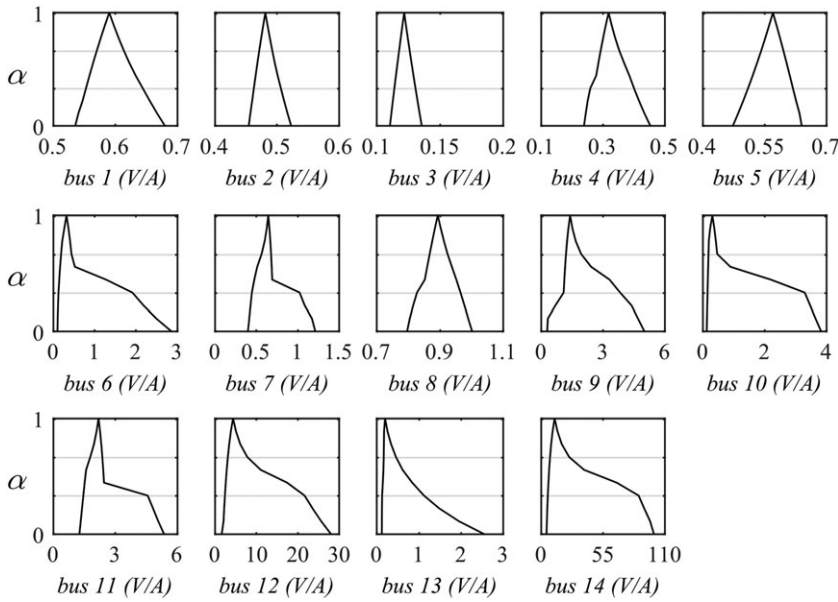
FIGURE 8 Possibility distributions of the 19th-order harmonic voltage per unit current

TABLE 5 Possibility measures and magnitude of resonances at 19th harmonic order

Bus	1	2	3	4	5	6	7	8	9	10	11	12	13	14
V/A_{max19}	-	-	-	0.45	-	2.86	1.21	1.0	5.01	3.82	5.36	28.1	2.55	**100.3**
$Pos(R_{19})$	0	0	0	0.5	0	0.33	0.33	0.16	0.33	0.33	0.33	0.33	0.33	0.33
$Nec(R_{19})$	0	0	0	0	0	0	0	0	0	0	0	0	0	0

Bold data indicates that bus 14 has the highest value of driving point impedance.
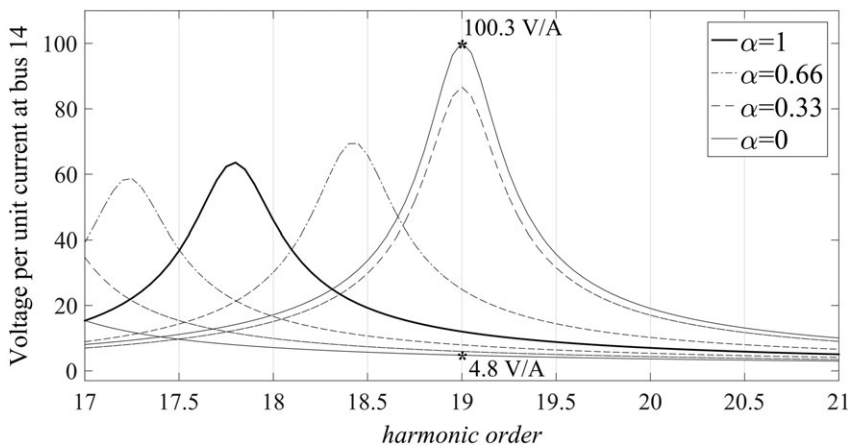

FIGURE 9 Possible frequency response of the network seen from bus 14

resonance magnitudes for the 13th and 17th harmonics. On the other hand, busses 3 and 8 have low risk of parallel resonance due to the harmonic filters connected to compensate for large nonlinear loads.

To highlight the capability of the possibility approach, when compared, for example, to a Monte Carlo-based approach, frequency scan results plotted in Figure 10 show that none of the 100 randomly generated profiles (assuming uniform probability distributions for the uncertain parameters) is tuned at the 19th harmonic order. In addition, there is no profile near the worst case of parallel resonance estimated with the possibility theory-based approach. A similar situation was observed with the results reported by Atkinson-Hope.[15,16] In that study, none of the plotted frequency scan profiles that were obtained using a "Variable Probability Method" achieves the worst possible case of parallel resonance, due to fact that only specific and predetermined load states were considered.
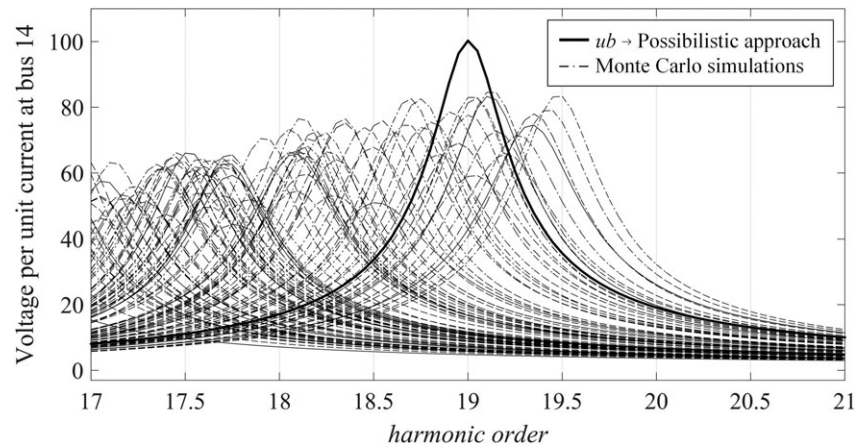
FIGURE 10 Frequency responses of the network, seen from bus 14, calculated with: the proposed possibility theory-based approach (bold line: upper boundary, "*ub*", of the 0-cut), and Monte Carlo simulations (dotted lines)

TABLE 6 Ranking of busses based on possibility, magnitude, and risk of resonance occurrence for 7th and 19th harmonics

	7th harmonic							19th harmonic						
Order	Bus	Pos	Nec	Bus	V/A$_{max}$	Bus	Risk	Bus	Pos	Nec	Bus	V/A$_{max}$	Bus	Risk
1	**4**	1	0.5	**14**	5.37	**14**	4.46	**4**	0.5	0	**14**	100.3	**14**	33.1
2	**5**	1	0.16	**12**	4.80	**12**	3.98	**14**	0.33	0	**12**	28.1	**12**	9.27
3	**7**	1	0.16	**13**	4.04	**9**	3.57	**12**	0.33	0	**11**	5.36	**11**	1.77
4	**9**	1	0.16	**9**	3.57	**13**	3.35	**11**	0.33	0	**9**	5.01	**9**	1.65
5	**10**	1	0	**10**	3.31	**10**	3.31	**9**	0.33	0	**10**	3.82	**10**	1.26
6	**6**	1	0	**11**	3.00	**4**	2.93	**10**	0.33	0	**6**	2.86	**6**	0.94
7	**2**	1	0	**4**	2.93	**5**	2.60	**6**	0.33	0	**13**	2.55	**13**	0.84
8	**14**	0.83	0	**5**	2.60	**11**	2.49	**13**	0.33	0	**7**	1.21	**7**	0.40
9	**12**	0.83	0	**6**	2.30	**6**	2.30	**7**	0.33	0	**8**	1.00	**4**	0.23
10	**13**	0.83	0	**1**	1.50	**7**	1.48	**8**	0.16	0	**4**	0.45	**8**	0.16
11	**11**	0.83	0	**7**	1.48	**2**	1.35	**1**	0	0	**1**	-	**1**	0
12	**1**	0.83	0	**2**	1.35	**1**	1.25	**2**	0	0	**2**	-	**2**	0
13	**3**	0.66	0	**3**	0.13	**3**	0.09	**3**	0	0	**3**	-	**3**	0
14	**8**	0	0	**8**	-	**8**	0.00	**5**	0	0	**5**	-	**5**	0

Finally, using results of the case study, it is concluded that the proposed approach allows for obtaining resonance points that represent the actual driving point impedance at the peak value, as the system load changes. Thus, resonance assessments performed with the possibility-based approach take into account all possible resonant points for a given period of study.

7 | CONCLUSION

A procedure based on possibility theory has been proposed in order to boost the capability of the frequency scan analysis in contexts where composition and magnitude of loads are known with uncertainty. In the outlined methodology, results of the possibilistic calculation of the driving point or transfer impedances are used to select, on a rational basis, specific values of the load parameters to carry out frequency scan calculations. It has been shown that the proposed methodology is a useful tool for detecting potential harmonic resonance. In particular, if a parallel resonance condition is detected, its maximum possible magnitude, as well as its associated possibility and necessity of occurrence, can be determined.

It is expected that index and rankings elaborated with this kind of possibilistic information concerning the harmonic behavior can be useful for comparing alternatives, regarding, for example, harmonic filter design, location and sizing of shunt compensation, etc.

ORCID

Andrés Arturo Romero Quete http://orcid.org/0000-0002-6530-852X
Joaquín Eduardo Caicedo Navarro http://orcid.org/0000-0003-2168-829X
Giuseppe Rattá http://orcid.org/0000-0003-3663-6310

REFERENCES

1. Xu W, Huang Z, Cui Y, Wang H. Harmonic resonance mode analysis. *IEEE Trans Power Deliv*. 2005;20(2 I):1182-1190. https://doi.org/10.1109/TPWRD.2004.834856

2. IEEE Recommended and Requirements for Harmonic Control in Electrical Power Systems. *IEEE Stand 519*-1992.

3. Das JC. *Power System Harmonics and Passive Filter Designs*. New Jersey: Wiley-IEEE Press; 2015. doi:https://doi.org/10.1002/9781118887059.

4. Bonner A, Grebe T, Gunther E, et al. Modeling and simulation of the propagation of harmonics in electric power networks. Part I: concepts, models, and simulation techniques. *IEEE Trans Power Deliv*. 1996;11(1):452-465. https://doi.org/10.1109/61.484130

5. Arrillaga J, Smith BC, Watson NR, Wood AR. *Power System Harmonic Analysis*. John Wiley & Sons; 1997.

6. Leite JC, Abril IP, De Lima Tostes ME, Limão De Oliveira RC. Frequency scan on a phase-coordinates frame for unbalanced systems. *Electr Pow Syst Res*. 2012;93:113-119. https://doi.org/10.1016/j.epsr.2012.07.013

7. Yang K, Bollen MHJ, Amaris H, Alvarez C. Decompositions of harmonic propagation in wind power plant. *Electr Pow Syst Res*. 2016;141:84-90. https://doi.org/10.1016/j.epsr.2016.06.029

8. Cho Y, Lee C, Hur K, et al. A framework to analyze the stochastic harmonics and resonance of wind energy grid interconnection. *Energies*. 2016;9(9). https://doi.org/10.3390/en9090700

9. Sainz L, Caro M, Caro E. Influence of Steinmetz circuit capacitor degradation on series resonance of networks. *Eur T Electr Power*. 2011;21(5):1689-1703. https://doi.org/10.1002/etep.514

10. Hong YY, Liao WJ. Optimal passive filter planning considering probabilistic parameters using cumulant and adaptive dynamic clone selection algorithm. *Int J Electr Power Energy Syst*. 2013;45(1):159-166. https://doi.org/10.1016/j.ijepes.2012.08.061

11. Hu H, Shi Q, He Z, He J, Gao S. Potential harmonic resonance impacts of PV inverter filters on distribution systems. *IEEE Trans Sustain Energy*. 2015;6(1):151-161. https://doi.org/10.1109/TSTE.2014.2352931

12. DIgSILENT GmbH. DIgSILENT PowerFactory. https://www.digsilent.de/en/power-quality-and-harmonic-analysis.html. Accessed February 19, 2018.

13. Operation Technology Inc. ETAP. https://etap.com/product/harmonic-frequency-scan-software. Accessed February 19, 2018.

14. Electric Power Research Institute EPRI. OpenDSS. http://smartgrid.epri.com/SimulationTool.aspx. Accessed February 19, 2018.

15. Atkinson-Hope G, Folly KA. Decision theory process for making a mitigation decision on harmonic resonance. *IEEE Trans Power Deliv*. 2004;19(3):1393-1399. https://doi.org/10.1109/TPWRD.2004.829142

16. Atkinson-Hope G, Amushembe H, Stemmet W. Effectiveness of filter types on efficiency in networks containing multiple capacitors and harmonic sources. In: 2014 Australasian Universities Power Engineering Conference, AUPEC 2014 - Proceedings; 2014. https://doi.org/10.1109/AUPEC.2014.6966492

17. Talaat N, Ilic M. A method for computing non-localized harmonic propagation and resonance in the electric energy systems. In: 41st North American Power Symposium, NAPS 2009; 2009. https://doi.org/10.1109/NAPS.2009.5483986.

18. Ribeiro PF. *Time-Varying Waveform Distortions in Power Systems*. New Jersey: John Wiley & Sons; 2009. doi:https://doi.org/10.1002/9780470746752.

19. Monjo L, Sainz L, Rull J. Statistical study of resonance in AC traction systems equipped with Steinmetz circuit. *Electr Pow Syst Res*. 2013;103:223-232. https://doi.org/10.1016/j.epsr.2013.05.014

20. Hu H, He Z, Wang K, Ma X, Gao S. Power-quality impact assessment for high-speed railway associated with high-speed trains using train timetable—part II: verifications, estimations and applications. *IEEE Trans Power Deliv*. 2016;31(4):1482-1492. https://doi.org/10.1109/TPWRD.2015.2472961

21. Zadeh LA. Fuzzy sets as a basis for a theory of possibility. *Fuzzy Set Syst*. 1978;1(1):3-28. https://doi.org/10.1016/0165-0114(78)90029-5

22. Dubois D, Prade H. Fuzzy sets in approximate reasoning, part 1: inference with possibility distributions. *Fuzzy Set Syst*. 1991;40(1):143-202. https://doi.org/10.1016/0165-0114(91)90050-Z

23. Dubois D, Prade H. Possibility theory. *Comput Complex*. 2012;2240-2252. https://doi.org/10.1007/978-1-4614-1800-9_139.

24. 31000 ISO. ISO 31000:2009 Risk management—principles and guidelines. In: *Risk Manag*; 2009.

25. Ross TJ. *Fuzzy Logic with Engineering Applications*. Third ed. New Jersey: John Wiley & Sons; 2010 https://doi.org/10.1002/9781119994374.

26. Romero AA, Zini HC, Rattá G. Modelling input parameter interactions in the possibilistic harmonic load flow. *IET Gener Transm Distrib*. 2012;6(6):528. https://doi.org/10.1049/iet-gtd.2011.0526

27. Burch R, Chang G, Hatziadoniu C, et al. Impact of aggregate linear load modeling on harmonic analysis: a comparison of common practice and analytical models. *IEEE Trans Power Deliv*. 2003;18(2):625-630. https://doi.org/10.1109/TPWRD.2003.810492

28. Romero AA, Zini HC, Rattá G, Dib R. Harmonic load-flow approach based on the possibility theory. *IET Gener Transm Distrib*. 2011;5(4):393. https://doi.org/10.1049/iet-gtd.2010.0361

29. Lasserre V, Mauris G, Foulloy L. A simple possibilistic modelisation of measurement uncertainty: the truncated triangular possibility distribution. In: 7th Int. Conference on Information Processing and Management of Uncertainty in Knowledge-Based Systems (IPMU'98). Vol 2. Paris; 1998:10-17.

30. Abu-hashim R, Burch R, Chang G, et al. Test systems for harmonics modeling and simulation. *IEEE Trans Power Deliv*. 1999;14(2):579-583. https://doi.org/10.1109/61.754106

31. Li W. *Risk Assessment of Power Systems: Models, Methods, and Applications*. Second ed. New Jersey: John Wiley & Sons; 2014 https://doi.org/10.1002/9781118849972.